Marius Engers*, Kent W. Stewart, Jan Liu and Peter P. Pott

Development of a realistic venepuncture phantom

Abstract: Venepuncture is one of the most common invasive procedures performed worldwide, however, complications still occur. Currently, commercial single layer silicone phantoms used for venepuncture training do not accurately imitate the geometry and mechanical properties seen in the various patient groups. This paper presents the development of a realistic artificial venepuncture phantom. Three multilayered tissue phantoms are developed simulating venepuncture sites of paediatric, adult and geriatric patients. Silicone materials of different stiffnesses were selected to imitate the epidermis, dermis, subcutaneous fat, muscle and superficial veins. Single-axis indentation tests were carried out on silicone samples and the multi-layered phantom inserts to characterize the material properties. The measured Young's moduli for the artificial dermis, fat and muscle show sufficient agreement with corresponding literature values. However, characterization of the complete phantom inserts showed stiffnesses four times larger than prior in-vivo studies. Future studies will work on developing a more comparable in-vivo study.

Keywords: Venepuncture, Tissue phantom, Indentation testing, Silicone molding

https://doi.org/10.1515/cdbme-2020-3104

1 Introduction

Blood sampling and the administration of medication has been used for decades in diagnostic and therapeutic health care procedures [1]. Venepuncture, the process of obtaining access to the superficial vessels of the venous system by an injection needle, is carried out thousands of times a day by medical professionals (phlebotomists) worldwide [2].

The anatomy of the venepuncture site varies from patient to patient due to age, sex and pre-existing diseases [3], which impedes the performance of a correct venepuncture without complications. Possible complications can occur, e.g. if the needle is inserted only partially into the vessel, causing leakage of blood and the formation of hematomas in the surrounding tissue [2]. In addition, improper needle insertion can lead to painful and severe damage when puncturing an artery or nerve instead of the vein [4].

Venepuncture is commonly performed by a clinician identifying the target blood vessel and then inserting a needle at the estimated appropriate angle and depth. Therefore, a proper and painless venepuncture depends on the experience and abilities of the phlebotomist. Furthermore, for a clinician to learn or continuously improve their skills of venepuncture without requiring patients there are commercially available artificial intravenous or venepuncture trainers imitating the anatomy of venepuncture site.

Venepuncture trainers usually consist of a rigid scaffolding structure containing tubes to simulate the blood vessels, covered with a softer skin-like sheathing. However, the significant disadvantage of such commercial models are the single-layered skin structure and scaffold do not adequately represent the actual multi-layered tissue composition at the venepuncture site and the different mechanical tissue properties. In addition, due to the unchangeable position and cross-section of the artificial veins, the typical anatomical variance and thus, the conditions to simulate different patients cannot be modified.

In order to enable a more realistic simulation of human tissue at the preferred puncture site of the forearm [1], a modular venepuncture phantom is investigated which considers a multilayer tissue structure with the individual mechanical properties. Three phantom inserts with different layer thicknesses and vein cross-sections enable the imitation of the typical structure of three different patient groups; paediatric, adult and geriatric.

This paper describes the development process of the venepuncture phantom, focusing on the characterization of the mechanical properties (Youngs modulus) of the individual layers and the complete phantom, and an appropriate layer structure geometry. Finally, the results of the characterization are described, and potential improvements are discussed.

***Corresponding author: Marius Engers:** Institute of Medical Device Technology, University of Stuttgart, Pfaffenwaldring 9, 70569 Stuttgart, Germany, e-mail: marius-engers@web.de
Kent W. Stewart, Jan Liu, Peter P. Pott: Institute of Medical Device Technology, University of Stuttgart, Stuttgart, Germany

2 Material and Methods

2.1 Venepuncture Site Characteristics

The preferred sites for venepuncture are veins of the volar side of the forearm at the cubital fossa, which typically comprises of the epidermis, dermis, subcutaneous fat with embedded veins and muscle. The outermost epidermis layer at the venepuncture site is very thin and shows no significant effects of age-related changes [5]. In contrast, the dermis, and the immediate subcutaneous fat increase with adulthood and then decrease at higher ages due to biochemical absorption processes [6] The blood vessels for venepuncture are embedded in the subcutaneous fat tissue [7] and the depth is defined by the superimposed skin layers. The muscle layer is required be sufficiently large for all phantom inserts to ensure that the rigid substrate below the insert has no negative influence on both the material characterization and needle insertion [8, 9].

The veins for venepuncture are the median cubital, basilica and cephalic vein. The diameter and wall thickness of these veins also change with age. The inner diameter of the veins increases until adulthood with a constant wall thickness to inner diameter ratio of 0.2 [1, 10]. The veins of geriatric patients have the same inner diameters as healthy adults however, the blood vessel walls also thin with age [11].

A summary of the geometric properties of the phantom inserts derived from literature are shown in Table 1.

In general, human tissue is characterized by a viscoelastic strain behaviour [12]. A method to characterise this is the Young's modulus obtained by measuring the stress-strain ratio for a purely elastic deformation at low strains (< 0.3) [12]. In regard to this, a summary of the Young's modulus found in literature can be seen in Table 1.

2.2 Artificial material characterisation

Due to the wide range of Young's Moduli, the comparative simple processing and long-term durability of the mechanical properties, silicone was selected as the tissue-imitating material. To determine the corresponding Young’s Moduli of the different artificial tissue types within the phantom, different samples were tested. The characterization of the materials was performed by indentation testing, similar to that described in [13]. A spherical indenter of brass, with a tip radius of 5 mm, was inserted into cylindrical silicone samples measuring the resulting force as a function of strain (see Figure 1). The indenting process and the force-displacement measurement was performed with the Quasar 25 materials testing machine (Galdabini (S.P.A.), Italy) provided the load cell TQ03.04.05 (Galdabini (S.P.A.), Italy) with a nominal value of 3 kN and a resolution of 0.15 N. Four different samples were created for characterisation of the individual

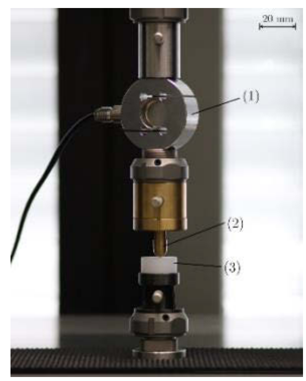

Figure 1: Set-up of the mechanical testing machine with the load cell (1), indenter (2) and sample in the test fixture (3).

tissue types. The different silicone materials used in the phantom were purchased from KauPo Plankenhorn e.K., Germany.

Each sample was periodically indented 6 times ($\varepsilon_{max} = 0.3$), with simultaneous force-displacement measurement. In addition, the test was performed at three different strain rates ($\dot{\varepsilon} = 0.1\ s^{-1}$ / $0.01\ s^{-1}$/$0.001\ s^{-1}$) derived from indentation tests on human skin or artificial viscoelastic materials from literature [13, 14, 15]. The Young’s Moduli, E, was determined by fitting the theoretical force-displacement curve, Eq. 1 proposed by Dimitriadis et al. [9], to the values obtained from indentation testing.

$$F = \frac{16E}{9}\sqrt{R\delta^3}(1 + 0{,}884\chi + 0{,}781\chi^2 + 0{,}386\chi^3 + 0{,}0048\chi^4) \qquad (1)$$

Table 1: Summary of the specified dimensions and material characteristics for the different artificial tissue types of the phantom inserts.

	Pediatric	Adult	Geriatric	Young’s Modulus in kPa	References
Thickness of epidermis in mm		0.15		1000 - 2000	[5, 14]
Thickness of dermis in mm	1.0	1.5	1.0	25 -75	[5, 15, 16, 17]
Thickness of fat in mm	1.5	2.0	1.5	1 - 5	[6, 15, 17]
Thickness of muscle in mm		> 5		75 - 100	[8, 9, 15]
Vein inner diameter in mm	1.5 – 3.0	4.0 – 6.0	4.0 – 6.0	2000- 3000	[1, 10, 18, 19, 20]
Vein wall thickness in mm	0.15 – 0.3	0.4 – 0.6	0.2 – 0.3		

This approximation formula considers the indenter tip radius R and the specimen height h. The height of the test specimen is included by the correction parameter χ, which needs to be calculated for each displacement δ. The curve was fit to minimise the root-mean-square error (RMSE) between the measured data and Dimitriadis's et. al model.

After the evaluation of the silicone samples, the inserts were manufactured by injection moulding. The mechanical characterization of the manufactured phantom inserts was then also performed under the same testing conditions. Since paediatric and geriatric inserts differ only in the size of the embedded veins, the indentation test was only performed the paediatric insert. The indentation was performed between the artificial veins, thus the stiffness of vein tubing had no influence on the determined total Young's modulus.

3 Results

The different cylindrical samples and complete inserts were tested, and the Young's moduli determined. The results for the strain rate $\dot{\varepsilon} = 0.01$ s^{-1} are shown in Table 2. In addition, Table 2 also shows the respective component mixing ratio of the silicones used. Figure 2 shows an example plot measured from the dermis silicone sample.

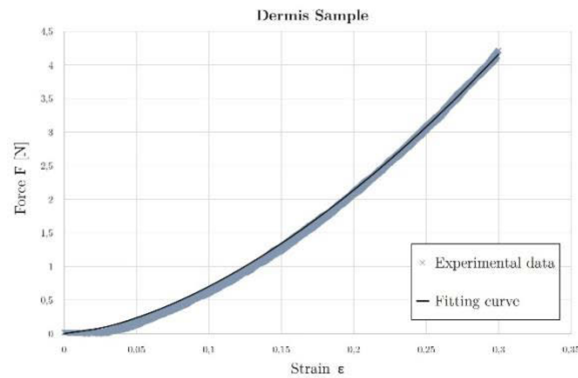

Figure 2: : Fitting of the curve according to Dimitriadis et al. [9] to the experimental loading data of the dermis sample.

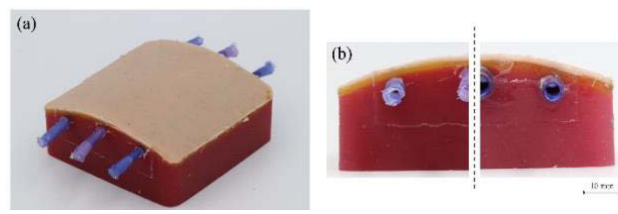

Figure 3 (a) Photograph of the complete infant insert and (b) comparison of the layer thickness of infant (left) and adult insert (right).

4 Discussion

The presented venepuncture phantom enables the imitation of the different patient groups with the anatomic variation in layer thickness and vein size (see Figure 3). For the described strain rate ($\dot{\varepsilon} = 0.01$ s^{-1}), the theoretical curve according to Dimitriadis et al. [9] show very good agreement to the experimental data for both the sample and the complete insert testing ($R^2 > 0.98$). The determined Young's moduli of the silicones imitating the human dermis ($E_{\text{Dermis}} = 65.20$ kPa), fat ($E_{\text{Fat}} = 3.60$ kPa), and muscle tissue ($E_{\text{Muscle}} = 96.60$ kPa), are within the desired range **(**Table 1**)**. For the epidermal layer and the blood vessels the selected silicone shows an insufficient Young's modulus ($E_{\text{E/V}} \approx 800$ kPa) not within the required range (1000 – 3000 kPa, Table 1). However, it was assumed that this had negligible influence on the overall phantom stiffness due to it them having relatively thin layers (Table 1).

After comparing the determined Young's moduli for the adult ($E_{\text{Adult}} = 79.20$ kPa) and paediatric/geriatric ($E_{\text{I/E}} = 77.50$ kPa) inserts with the values of in-vivo studies ($E = 10$-20 kPa) [13, 15], it becomes apparent that differ considerably and are about four times higher than values presented in these studies. This could indicate that the Young's moduli defined of muscle, fat and dermis silicone are too high or the thickness of the layers are incorrect and should be further investigated. However, a fair comparison between the penetration tests performed in this work and those from the literature is difficult due to the different test conditions such as indenter geometry, penetration velocity and/or the selection of the mathematical model for the determination of the Young's modulus. Thus, further evaluation of the developed inserts should be first performed by comparison with in-vivo experiments performed in an identical manner.

Table 2: Average values of Young's modulus of the different silicone specimen from indentation test with a strain rate of $\dot{\varepsilon} = 0.01\text{s}^{-1}$. The component mixture for the fat layer was extended by adding a third component (slacker) to adjust the actual Young's modulus.

Tissue type	Calculated Young's Modulus in kPa	R^2	Material	Mixing ratio A:B
Epidermis/Vein	796.8	0.996	Dragon Skin 30	1:1
Dermis	65.2	0.998	Ecoflex 0030	1:1
Fat	3.6	0.983	Ecoflex 0050 + Slacker	1:1:1*
Muscle	96.6	0.997	Ecoflex 0050	1:1
Complete insert	77.5 (Paediatric /Geriatric)/79.2 (Adult)	0.995	-	-

From Figure 2 it appears that the layer thicknesses of silicone are consistent and at the defined value. However, a proper determination of the manufactured layer thicknesses and the cross-section of the artificial veins was not carried out. Thus, in order to assess the usability of the manufacturing process and to relate the mechanical characteristics of the phantom inserts to the geometric parameters, the layer thicknesses and the cross-section of the veins should be determined, e.g. through ultrasound imaging.

Overall, a realistic venepuncture site phantom was developed with four different layers of varying mechanical properties and layer heights to imitate three different age groups. Future work will focus on a direct comparison to in-vivo experiments and the qualitative analysis by medical professionals.

Author Statement

Research funding: The author state no funding involved. Conflict of interest: Authors state no conflict of interest.

Reference

[1] World Health Organization, Hrsg., WHO Guidelines on Drawing Blood: Best Practices in Phlebotomy.

[2] B. S. Sorensen, S. P. Johnsen und J. Jorgensen, „Complications related to blood donation: a population-based study,“ Vox sanguinis, Bd. 94, Nr. 2, p. 132–137, 2008.

[3] Hristo Petrov Dobrev, „Study of human skin mechanical properties by mean of Cutometer,“ Folia Medica, 2002.

[4] H. J. Kim, S. K. Park und S. H. Park, „Upper limb nerve injuries caused by intramuscular injection or routine venipuncture,“ Anesthesia and Pain Medicine, Bd. 12, Nr. 2, p. 103–110, 2017.

[5] Sieglinde Neerken, Gerald W. Lucassen, Marielle A. Bisschop, Egbert Lenderink und Tom A. M. Nuijs, „Characterization of age-related effects in human skin: A comparative study that applies confocal laser scanning microscopy and optical coherence tomography,“ Journal of Biomedical Optics, Bd. 9, Nr. 2, p. 274–281, 2004.

[6] Catherine Escoffier, Jean de Rigal, Annie Rochefort, Régis Vasselet, Jean-Luc Léveˆque und Pierre G. Agache, „Age-related mechanical properties of human skin: An in vivo study,“ Journal of Investigative Dermatology, Bd. 93, Nr. 3, p. 353–357, 1989.

[7] Robert F. Rushmer, Konrad J. K. Buettner, John M. Short und George F. Odland, „The Skin,“ Science, Bd. 154, Nr. 3747, p. 343–348, 1966.

[8] Thomas A. Krouskop, Thomas M. Wheeler, Faouzi Kallel, Brian S. Garra und and Timothy Hall, „Elastic Moduli of Breast and Prostate Tissues under Compression“.

[9] Emilios K. Dimitriadis, Ferenc Horkay, Julia Maresca, Bechara Kachar und Richard S. Chadwick, „Determination of Elastic Moduli of Thin Layers of Soft Material Using the Atomic Force Microscope,“ Biophysical Journal, Bd. 82, Nr. 5, p. 2798–2810, 2002.

[10] H.-C. Pape, A. Kurtz und S. Silbernagl, Physiologie, 8., unveränderte Auflag Hrsg., Stuttgart: Thieme, 2018.

[11] R. Schelper, „The Aging Venous System,“ Journal of the Association for Vascular Access, Bd. 8, Nr. 3, p. 8–10, 2003.

[12] Guy Lamouche, Brendan F. Kennedy, Kelsey M. Kennedy, Charles-Etienne Bisaillon, Andrea Curatolo, Gord Campbell, Valérie Pazos und David D. Sampson, „Review of tissue simulating phantoms with controllable optical, mechanical and structural properties for use in optical coherence tomography,“ Biomedical Optics Express, Bd. 3, Nr. 6, p. 1381, 2012.

[13] J. Jachowicz, R. McMullen und D. Prettypaul, „Indentometric analysis of in vivo skin and comparison with artificial skin models,“ Skin Research and Technology, Bd. 13, Nr. 3, p. 299–309, 2007.

[14] M. Geerligs, Breemen, van, L.C.A., G.W.M. Peters, P.A.J. Ackermans, F.P.T. Baaijens und C.W.J. Oomens, „In vitro indentation to determine the mechanical properties of epidermis,“ Journal of Biomechanics, Bd. 44, Nr. 6, p. 1176–1181, 2011.

[15] C. Pailler-Mattei, S. Bec und H. Zahouani, „In vivo measurements of the elastic mechanical properties of human skin by indentation tests,“ Medical Engineering & Physics, Bd. 30, Nr. 5, p. 599–606, 2008.

[16] F. M. Hendriks, D. Brokken, Van Eemeren, J. T. W. M., C. W. J. Oomens, F. P. T. Baaijens und Horsten, J. B. A. M., „A numerical-experimental method to characterize the non-linear mechanical behaviour of human skin,“ Skin Research and Technology, Bd. 9, Nr. 3, p. 274–283, 2003.

[17] J.-L. Gennisson, T. Baldeweck, M. Tanter, S. Catheline, M. Fink, L. Sandrin, C. Cornillon und B. Querleux, „Assessment of elastic parameters of human skin using dynamic elastography,“ IEEE Transactions on Ultrasonics, Ferroelectrics and Frequency Control, Bd. 51, Nr. 8, p. 980–989, 2004.

[18] F. Pukacki, T. Jankowski, M. Gabriel, G. Oszkinis, Z. Krasinski und S. Zapalski, „The Mechanical Properties of Fresh and Cryopreserved Arterial Homografts,“ European Journal of Vascular and Endovascular Surgery, Bd. 20, Nr. 1, p. 21–24, 200.

[19] Harunobu Shima, Kohsuke Ohno, Ken-ich Michi, Kaoru Egawa und Reiji Takiguchi, „An anatomical study on the forearm vascular system,“ Journal of Cranio-Maxillofacial Surgery, Bd. 24, Nr. 5, p. 293–299, 1996.

[20] Simon A Mahler, Greta Massey, Liliana Meskill, Hao Wang und Thomas C Arnold, „Can we make the basilic vein larger? maneuvers to facilitate ultrasound guided peripheral intravenous access: a prospective cross-sectional study,“ International journal of emergency medicine, Bd. 4, Nr. 1, 2011.